

**Agenda item:** 8.1.4.1  
**Source:** Qualcomm Incorporated  
**Title:** Waveform Candidates  
**Document for:** Discussion/Decision

---

## 1 Introduction

In RAN#71, the technology study item for 5G new RAT (NR) has been approved [1]. For the New Radio Access Technology (NR), there is potential to improve the waveform design to efficiently multiplex different services while optimize for the specific requirements of each service, respectively.

The typical use cases, as well as their specific requirements, for potential waveform optimization has been listed in [3]. Several evaluation metrics for waveform evaluation and comparison are listed in [4]. In this contribution, we discuss several waveform candidate proposals from literature to be further evaluated for various service/deployment scenarios for the new RAT.

---

## 2 Waveform Candidates

### 2.1 Single carrier waveforms

Single carrier modulations have been widely used in cellular systems such as GSM, CDMA2000 and UMTS WCDMA. Due to their time domain symbol sequencing, they typically provide low peak-to-average power ratio (PAPR), leading to higher PA efficiency and extended battery life. This makes single carrier waveform particularly suited for use cases such as mMTC (i.e. WAN IoT) where battery power and coverage extension are the main optimization goals.

On the other hand, single carrier waveforms suffer link degradation under frequency selective channels, and typically require the use of equalizer to achieve high spectral efficiency in the presence of multipath.

#### 2.1.1 Constant envelope waveform

The simplest solution to high transmit efficiency is to employ a constant envelope waveform. This allows almost any PA to be run at saturation point without clipping or a need for pre-compensation or post-compensation to account for clipping. The drawback to this mechanism however has been the inefficiency from a capacity standpoint relative to quadrature amplitude modulation [12], but for the class of applications where high data rate is not required, a constant envelope waveform is more desirable since it achieves the highest PA efficiency.

The most popular constant envelope waveforms including minimum-shift-keying (MSK) [20][21] and Gaussian minimum-shift-keying (GMSK) [22], belong to the class of continuous phase frequency-shift-keying (CPFSK) signals. MSK was adopted by the IEEE 802.15.4 standard [23], which provides the physical layer platform for ZigBee. GMSK is also used in GSM, Bluetooth, and BT-LF.

It is well known that MSK can equivalently be viewed as Offset-QPSK with sinusoid pulse shaping, which provides efficient modulation and demodulation. Notice that a differential encoder is inserted before the modulator to avoid error propagation at the demodulator[21]. This also helps to simplify the modulator, as the differential encoder and differential decoder cancel each other.

GMSK is a variant of MSK, where a Gaussian-filtered version of the information sequence is applied to an MSK modulator. The Gaussian filter helps to increase the spectral efficiency of the MSK, with the penalty of inter-symbol interference. Note that with the introduction of Gaussian filtering, the GMSK signal can no longer be viewed as Offset-QPSK. Typical

receivers for GMSK use a linear approximation of the GMSK pulses [24][25] and treat the modulation as a sum of pulse amplitude modulation (PAM) signals. Based on this approximation, one can use the well-known Viterbi detector as a demodulator. Notice that lower complexity demodulator for GMSK is typically used for low power devices, such as BTLE.

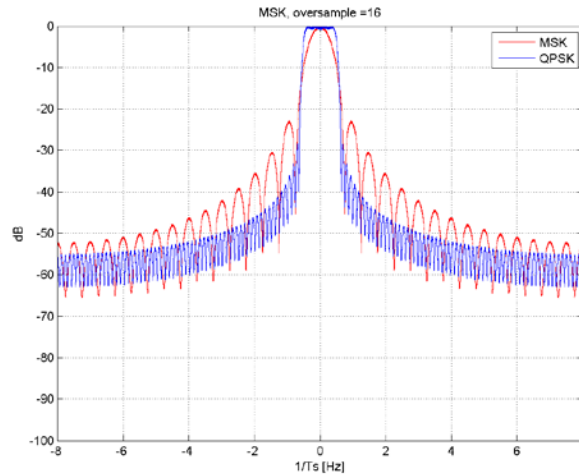


Figure 2-1 MSK PSD

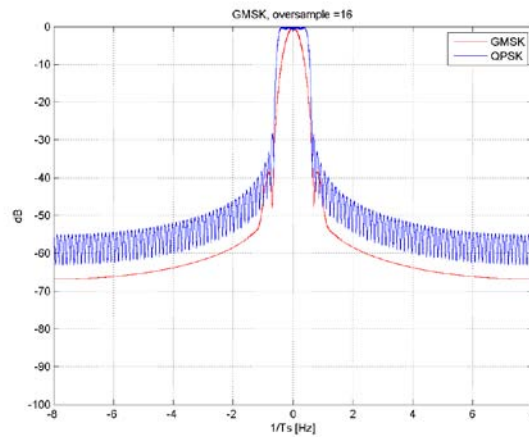


Figure 2-2 GMSK PSD

In summary, we conclude the following for constant envelope:

Table 2-1 Summary of constant envelope waveform

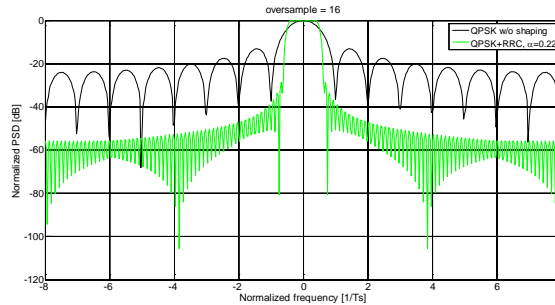
|   | statement                      | comments   |
|---|--------------------------------|--|
| 1 | High PA efficiency             | 0dB PAPR gives highest PA efficiency   |
| 2 | Reasonable receiver complexity | Comparable with SC-QPSK  |
| 3 | Comparable ACLR as SC-QAM      | MSK: worse than SC-QPSK w/ RRC pulse shaping<br>GMSK: better than SC-QPSK w/ RRC pulse shaping |

|   |                         |   |
|---|-------------------------|---|
| 4 | Low spectral efficiency | MSK: maximal 1bit/sym<br><br>GMSK: maximal 1bit/sym |
|---|-------------------------|---|

### 2.1.2 Single carrier QAM

As mentioned before, higher orders of QAM can be used to achieve higher spectral efficiency with a single carrier waveform. The most common waveform used in 3G cellular networks (e.g. UMTS, CDMA2000, 1xEV-DO) is single carrier CDMA with QAM modulation.

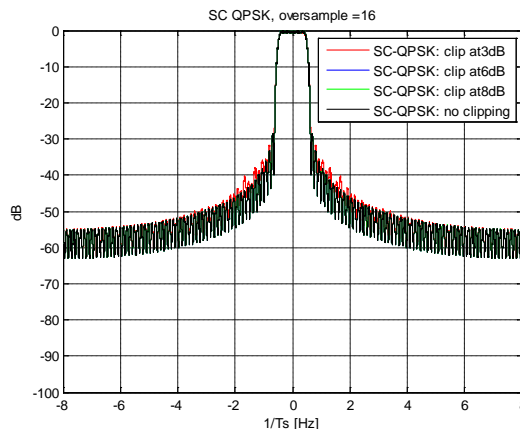
Specifically, when QPSK modulation is chosen, it gives a constant amplitude waveform with 0dB PAPR. In practice, however, single carrier modulation is typically followed by a time-dispersive transmit pulse shaping filter that is more localized in frequency domain, in order to reduce out of band (OOB) leakage and meet adjacent channel leakage ratio (ACLR) requirements. Figure 2-3 illustrates the power spectral density (PSD) of single carrier QPSK modulation with and without transmit pulse shaping. As a result, a matched filter is also introduced at the receiver side to maximize the SNR. In order to remove intersymbol interference (at least for a frequency flat channel), the pulse shaping filter is typically selected as a half-Nyquist filter, i.e. the concatenated response of the transmit and receiver filters has the Nyquist property. Specifically, in Figure 2-3, plots the PSD for a root-raised cosine filter with rolloff factor  $\alpha = 0.22$ , as used in WCDMA.



**Figure 2-3 Single carrier QPSK PSD**

Notice that with transmit pulse shaping, the transmitted waveform is no longer constant envelope and has  $>0$  dB PAPR. In Figure 2-4, we illustrate the PSD of single carrier QPSK with different clipping thresholds above the average power. Figure 2-6 shows the EVM corresponding to different clipping thresholds.

Several enhancements can be applied to further reduce the PAPR, such as  $\pi/4$ -QPSK, which introduces a rotation of  $\pi/4$  between even and odd constellations and therefore eliminates any path through the origin (i.e., zero-crossings). In UMTS, HPSK scrambling is used to eliminate any path through the origin between any pair of chips with index  $(2k, 2k + 1)$ . This approach relies on the fact that a spreading factor of at least 2 is used for spreading the modulated symbols.



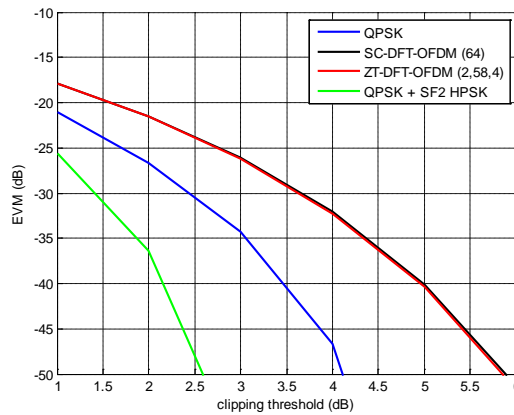
**Figure 2-4 QPSK PSD with Clipping at Transmitter**

Figure 2-5 compares the PAPR of several single carrier waveforms with QPSK modulation, some of them will be discussed in later sections. Notice that except for the constant envelope waveforms discussed in section 2.1.1, single carrier QPSK with HPSK gives the best PAPR among those popular single carrier waveforms we evaluated. This partly explains the observations from Figure 2-6 where single carrier QPSK gives lower EVM compared to the DFT-spread OFDM waveforms discussed in section 2.1.4 and 2.1.5.

It should be noted that the PAPR and clipping shown here do not reflect multiple user multiplexing such as code-division multiplexing. When these are applied the PAPR can be much higher than shown, as reported in [7].



**Figure 2-5 PAPR of single carrier waveforms**



**Figure 2-6 EVM of single carrier waveforms**

Additionally, two natural approaches can be pursued to achieve wider bands, that is by increasing the sample rate, or by providing a separate single carrier on an adjacent channel. As can be seen in Figure 2-4, the pulse shaping filter can be designed to provide sufficient adjacent channel suppression for that each channel can achieve its desired peak rate. This latter approach serves the basis for 3G multicarrier approaches, such as EV-DO Revision B or Dual-Carrier HSDPA.

In summary, we conclude the following for SC-QAM:

**Table 2-2 Summary of SC-QAM**

|   | statement                  | comments  |
|---|----------------------------|---|
| 1 | Good PA efficiency and EVM | Only worse than constant envelope waveforms, especially with low PAPR scrambling. |

|   |           |                                   |
|---|-----------|-----------------------------------|
| 2 | Good ACLR | Need to use pulse shaping filter. |
|---|-----------|-----------------------------------|

### 2.1.3 Single Carrier Frequency Domain Equalization

One important aspect to achieving higher spectral efficiency with single carrier QAM in the presence of multipath fading is to employ a good equalization algorithm. In many cases, this is left to the design of the receiver and the complexity which can be afforded depending on implementation. Although there are well-known time-domain algorithms such as fractionally spaced equalization, RAKE, and adaptive equalization, it is a common misconception that computationally efficient frequency domain equalization is relegated to OFDM-only waveforms. In fact, to the contrary, single carrier can be implemented with frequency domain equalization, and the construction of a block-based transmission scheme which includes a cyclic prefix is often referred to formally as SC-FDE [13]. Such a scheme is illustrated in Figure 2-7. A standard that includes this waveform is 802.11ad, which is an unlicensed mmW technology at 60GHz, and commercial implementations using this waveform have been released by Qualcomm Atheros.

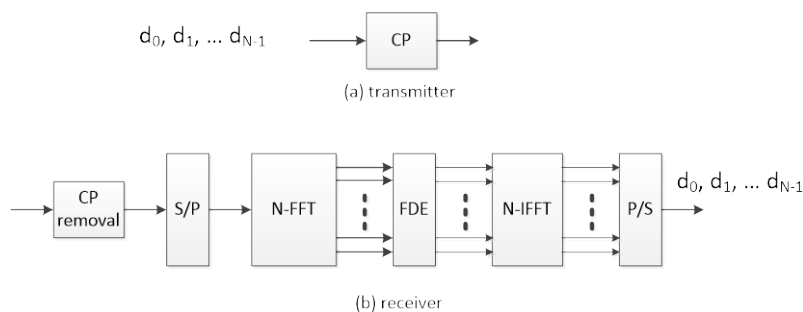


**Figure 2-7 SC-FDE modulator and demodulator**

In summary, SC-FDE has comparable pros/cons as SC-QAM, except offering convenient implementation of FDE at receiver, at the cost of spectral efficiency loss due to CP.

### 2.1.4 Single Carrier DFT-spread OFDM

A variation on SC-FDE is DFT-spread OFDM, where the time domain QAM is transformed with an M-point DFT which is used to modulate a different set of tones across a larger IFFT which transforms this signal back to time domain. If the size M is equal to the size of the IFFT, we have the original SC-FDE of the previous section.

The main purpose of DFT-spread OFDM is the flexibility in allocating different bandwidth to multiple users orthogonally in frequency domain. When this waveform is combined with frequency multiplexing, this is then typically referred to as SC-FDMA. There are two common ways for assigning bandwidth in SC-FDMA:

- Localized SC-FDMA (LFDMA): each user is assigned contiguous sub-carriers. An example of this approach is in the LTE uplink data and uplink control channels.
- Interleaved SC-FDMA (IFDMA): each user is assigned non-contiguous sub-carriers that are uniformly distributed over the entire band. Although not contiguous, the equal distance between the sub-carriers still keeps the IFFT output a single carrier waveform. An example of this approach is in the uplink SRS of LTE.

Since each user's assigned sub-carriers spans the entire band, IFDMA potentially can achieve better frequency diversity compared to LFDMA. However, channel interpolation in frequency domain can be more difficult in IFDMA depending on the coherence bandwidth of the channel.

As with SC-FDE, adding a cyclic prefix to the waveform allows simple and obvious implementation of a frequency domain equalizer at the receiver. The M-point DFT precoding helps to retain the single carrier property after the N-point OFDM for the waveform synthesis, thus resulting in lower PAPR than the regular OFDM waveform discussed in the next section. The reduced PAPR can be translated to better efficiency if the PA is run with less backoff, though less ideal compared to other waveforms.

Another important benefit of SC-FDMA is the low inter-carrier interference which can be provided when there is tight synchronization. Mathematically, this intercarrier interference becomes zero with perfect synchronization since the set of subcarriers used by each M-point DFT has a null at the subcarriers of any other M-point DFT. This is not always the case for other frequency domain multiplexing schemes such as the use of RRC filtering to separate adjacent subchannels, as shown in Figure 2-3. It should be noted however, that unlike RRC filtering which continuously interpolates across all QAM symbols, since SC-FDMA is a block based waveform technique there will be discontinuities between blocks. However, this can be mitigated with weighted-overlap-and-add (WOLA) which will be discussed in more details in section 2.2.2. The improvements from WOLA to the emissions are shown in Figure 2-8

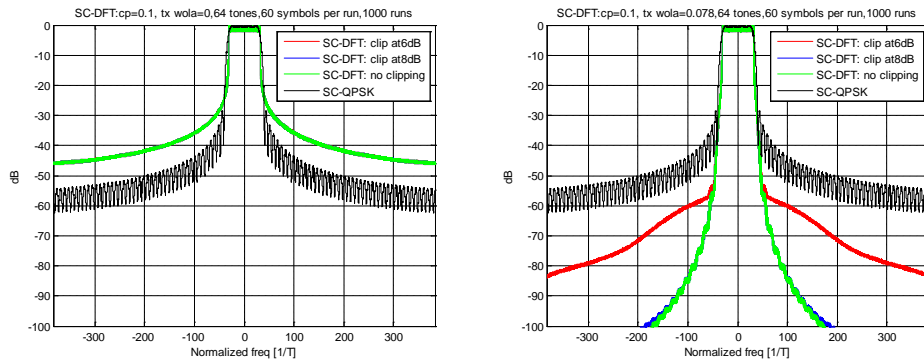


**Figure 2-8 PSD of DFT-spread OFDM without WOLA (left), with WOLA (right)**

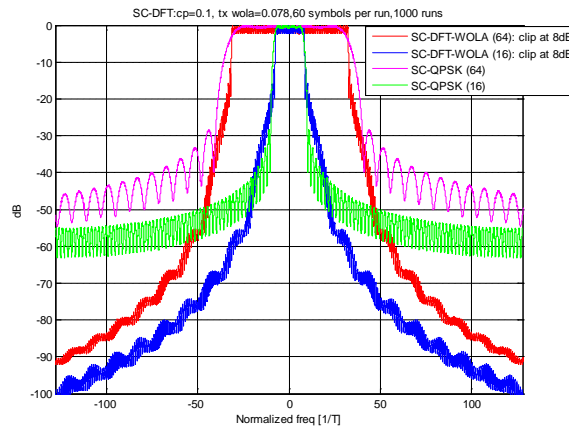


**Figure 2-9 PSD of DFT-spread OFDM for different number of tones**

In summary, we can conclude the following for SC DFT-spread OFDM:

**Table 2-3 Summary of SC DFT-spread OFDM**

|   | statement                           | comments   |
|---|-------------------------------------|--|
| 1 | Support dynamic spectrum allocation | More flexible than SC-QAM with efficient DFT/IFFT implementation |
| 2 | Handles multipath with FDE          | CP convert channel to circular convolution                       |
| 3 | Worse PAPR/EVM than SC-QPSK         | However, better than OFDM  |

|   |                         |                       |
|---|-------------------------|-----------------------|
| 4 | Better ACLR than SC-QAM | When Tx-WOLA is used. |
|---|-------------------------|-----------------------|

## 2.1.5 Zero-Tail DFT-OFDM

There was a recent publication on zero-tail DFT-spread OFDM [27] which is a variant of the single carrier DFT-spread OFDM discussed in section 2.1.4. The main change is that the regular cyclic prefix is replaced by zero symbols padded to the data input to the DFT precoding, as shown in Figure 2-10.

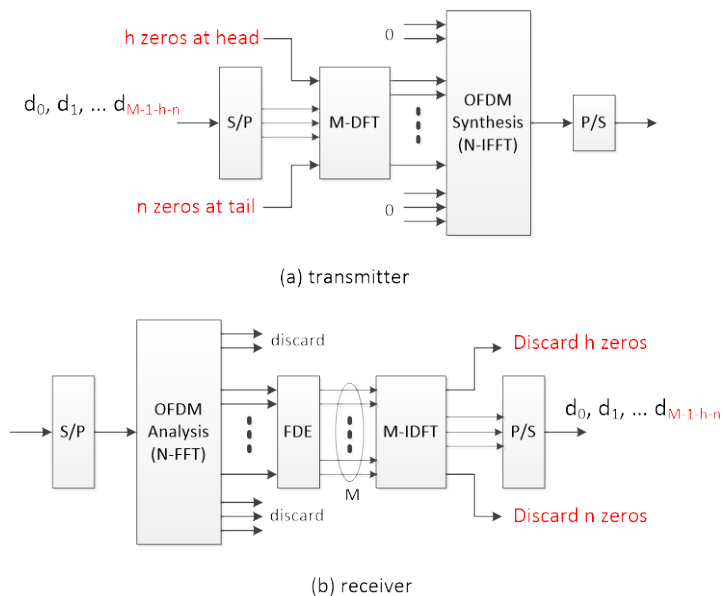


**Figure 2-10 Zero-tail DFT-spread OFDM modulator & demodulator**

It was claimed [27] that the zero-tail insertion has the following benefits:

- The length of the zero tail can be variable, depending of the channel delay spread and propagation delay on a per-user basis, rather than a fixed CP length across the network. This could potentially reduce the overhead for some users.
- The OOB leakage can be suppressed due to the zero padding, which smoothens the transitions between adjacent symbols.
- Zero tail can potentially reduce the overhead associated with RF beam switch.

When comparing DFT-spread OFDM with zero-tail, it would seem there is a slight improvement in link performance with the zero tail guard optimization. However, in reality it is not sufficient to only change the CP or guard to handle all delay spreads, but the subcarrier spacing (and thus block length) should also be scaled to best address the delay spread and channel selectively. Therefore, for the same block size and subcarrier spacing, the zero tail guard optimization might only benefit up to 7%, if we consider the CP overhead in LTE. Moreover, there would be additional signaling overhead to support the added control loop complexity for zero-tail.

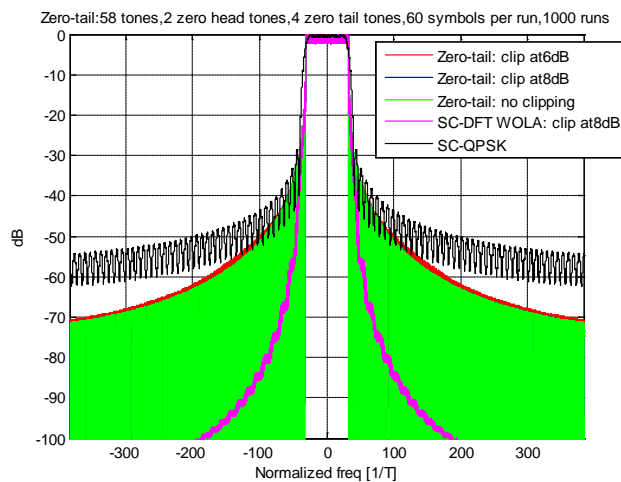
Figure 2-5 and Figure 2-6 compare the PAPR and EVM of ZT DFT-spread OFDM to other single carrier waveforms. Notice that the part of post-IFFT samples corresponding to the inserted zero tails are not part of useful signal, we exclude it from average power calculation. As expected, the ZT DFT-spread OFDM gives comparable PAPR and EVM as the regular DFT-spread OFDM waveform.

Figure 2-11 compares the PSD of ZT DFT-spread OFDM with single carrier QPSK. It worse than single carrier QPSK above -50dB, but decays faster at from -50dB. The opposite case is true when compared against SC-FDMA from the previous figure.

Based on the above analysis, we can summarize the following for ZT DFT-spread OFDM:

**Table 2-4 Summary of ZT SC DFT-spread OFDM**

|   | statement   | comments  |
|---|---|---|
| 1 | improvement to spectral efficiency of some users [27] | Depending of the variation of delay spread among users. Up to 7% (i.e., remove current CP overhead) |
| 2 | Better OOB suppression than DFT-spread OFDM [27]      | But worse than DFT-spread OFDM with WOLA.   |
| 3 | Extra signaling overhead                              | UE need to know the delay spread of the channel.  |
| 4 | Can't multiplex with OFDM users within same band.     | The symbol duration is different from the OFDM users due to the lack of CP                          |



**Figure 2-11 PSD of zero-tail DFT-spread OFDM with Clipping at Transmitter**

## 2.2 OFDM-Based Multi-carrier waveforms

Multi-carrier waveforms can generally be represented by the following expression

$$y(n) = \sum_{k=-\infty}^{\infty} \sum_{m=0}^M d_{k,m} \cdot p(n - kM) \cdot e^{j2\pi mF(n-kM)}$$

### Equation 2-1

where  $p(n)$  is the prototype filter, and  $e^{j2\pi mF(n-kM)}$  represents the frequency shifter corresponding to the  $m$ -th sub-carrier,  $k$  is the data symbol index within each carrier, and  $n$  is discrete time index in the digitally (possibly oversampled) domain. A general implementation is illustrated in Figure 2-12. The multi-carrier waveform can be further enhanced by inclusion of the band-pass filter  $b(n)$  to suppress out-of-band (OOB) leakage.

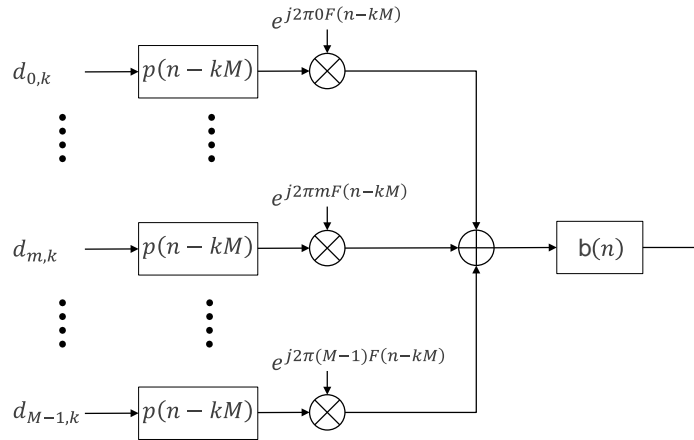


**Figure 2-12 Multi-carrier waveform synthesis**

Although this seems similar to schemes such as EV-DO Revision B or DC-HSDPA as discussed in Section 2.1.2, in this section we will consider only those constructions such that subcarriers may have frequency overlap with neighboring subcarriers but are actually zero at the perfect subcarrier sampling in frequency domain. The most commonly deployed version of this approach is OFDM, and thus we call related waveforms in this section OFDM-based multicarrier waveforms.

The various OFDM-based multi-carrier waveforms we will discuss in the next sections are differentiated amongst themselves based on the optimization differences of the two filters  $p(n)$  and  $b(n)$ . Specifically,

- $p(n)$  is typically implemented through time domain **windowing**, which corresponds to manipulating the pulse shaping of each sub-carrier in frequency domain. As we will see, the FBMC discussed in section 2.2.6 and the WOLA in section 2.2.2 can be equivalently viewed as this approach.
- $b(n)$  is typically implemented through time domain **filtering**, which corresponds to apply a frequency domain band-pass window over a block of contiguous sub-carriers. The UFMC in section 2.2.3, FCP-OFDM in section 2.2.4 and F-OFDM in section 2.2.5 belongs to this category.

## 2.2.1 CP-OFDM

The CP-OFDM waveform is the most widely used multi-carrier waveform in existing broadband wireless standards, including 3GPP LTE and IEEE 802.11, due to its many attractive features:

- Efficient implementation using FFT/IFFT
- Rather straightforward application of MIMO technology over non-flat channel for high spectrum efficiency with the use of the CP
- Simple FDE per subcarrier for non-flat channel
- Dynamically allocate bandwidth to users

CP-OFDM waveform can be synthesized as a simple special case of Figure 2-12 by

- Setting the prototype filter  $p(n)$  as rectangular pulse
- bypassing  $b(n)$

Such simplifications allow efficient implementation of the modulator and demodulator using FFT and IFFT.

One early advantage of OFDM over single carrier methods is the link performance degradation in frequency selective fading channels [26], however with more evolved receiver designs it is possible for SC-FDE and related variants to perform comparably even before PA non-linearity is introduced [13]. Another more important differentiator is in the signal and user multiplexing afforded by OFDM over single carrier, which is particularly important for enabling such features as MIMO spatial multiplexing. For instance, pilot placement for channel estimation across different multiplexed users can be more

flexible across the entire OFDM time-frequency grid as opposed to single carrier or even DFT-spread OFDM. However, at lower spectral efficiencies without spatial multiplexing, single carrier and DFT-spread OFDM can be more appropriate for scheduled transmission with lower order modulation (e.g. QPSK) from power limited devices.

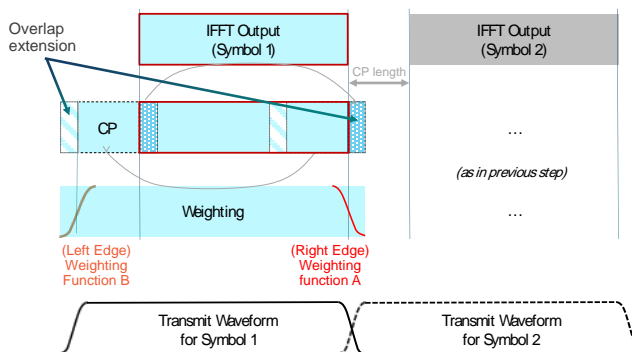
One reported drawback of the CP-OFDM waveform itself (i.e. without additional transmit processing such as WOLA) is the rather poor frequency localization due to the rectangular prototype filter  $p(n)$ . The slowly decaying OOB leakage could potentially cause interference to the adjacent band. It also leads to in-band interference whenever there is frequency offset between users. Figure 2-14 shows the PSD of CP-OFDM waveform with 12 contiguous data tones. The CP length is set to be roughly 10% of the OFDM symbol length. The PAPR is shown later in Figure 2-21 and is noticeably higher than single carrier waveforms.

## 2.2.2 CP-OFDM with WOLA

In CP-OFDM with weighted overlap and add (WOLA), the rectangular prototype filter  $p(n)$  is replaced by pulse with soft edges at both sides, which results in much sharper side-lobe decay in frequency domain. The soft edges at the beginning and end of the filter response effectively gives a better contained prototype filter in frequency domain. Therefore, CP-OFDM with WOLA is a special case of Figure 2-12 with:

- improving the prototype filter  $p(n)$  such that it has better frequency response than rectangular filter used in regular CP-OFDM
- bypassing  $b(n)$ .

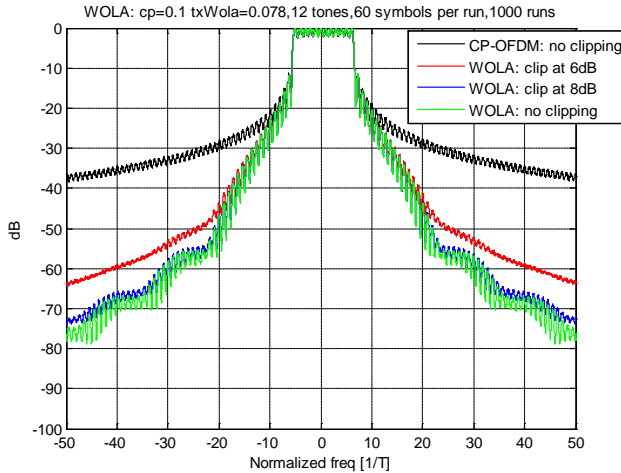
In practice, the better contained frequency response is achieved by using a time domain windowing approach which add soft edges to the cyclic extension of OFDM symbol, as shown in Figure 2-13. Although the edges further expand each symbol, the overhead is still the same as CP-OFDM waveform, since adjacent symbols are overlapped in the edge transition region as shown in Figure 2-13.



**Figure 2-13 WOLA at transmitter with CP-OFDM**

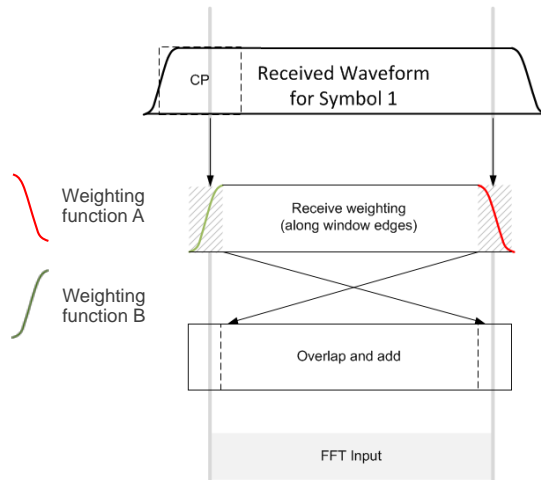
The shape of the window (or edge) in time domain determines the frequency response of the prototype filter. Several types of windowing have been evaluated in literature [30] with different tradeoffs between the width of the main lobe and suppression of the side lobes. In general, a raised-cosine edge seems to offer a good compromise with straightforward implementation.

Figure 2-14 illustrates the PSD of CP-OFDM with WOLA at the transmitter. Notice that OOB suppression is substantially better than the CP-OFDM. The PAPR of CP-OFDM with Tx-WOLA is comparable to regular CP-OFDM, as shown in Figure 2-21.



**Figure 2-14 CP-OFDM with Tx-WOLA PSD with clipping**

In addition to applying WOLA at the transmitter to reduce the OOB leakage from the signal, we notice that WOLA can be similarly applied at the receiver to suppress other users' interference as well. When users are asynchronous, the soft edges applied at the receiver help to reduce other user interference resulting from the mismatched FFT capture window. The Rx-WOLA processing is illustrated in Figure 2-15.



**Figure 2-15 CP-OFDM WOLA processing at the receiver**

To illustrate the effect of suppressing interference from asynchronous users by using Rx-WOLA, we compare the OOB leakage from an adjacent interferer with random offset in Figure 2-16. In the simulation, two users with 12 tones are adjacent to each other, and FFT capture window is aligned to the desired user's signal. We insert random offset between the two users, and averaged the PSD of the interferer over 1000 runs. As shown in Figure 2-16, the interference from the asynchronous neighboring user is noticeably higher when there is Rx-WOLA.

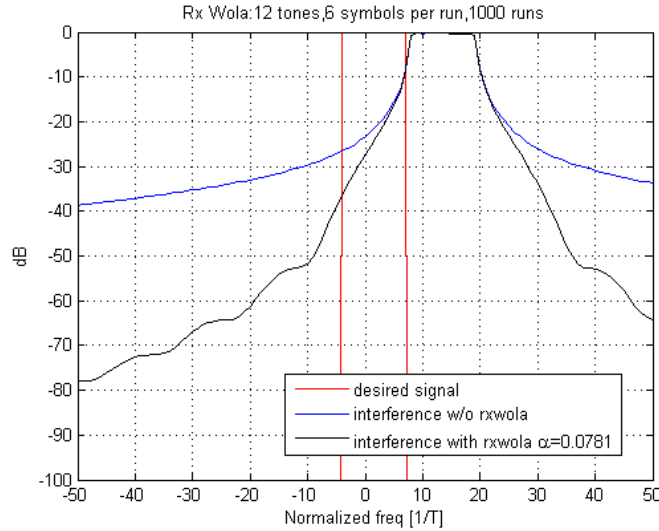


**Figure 2-16 PSD with CP-OFDM Tx and Rx WOLA**

In summary, WOLA is a very attractive pulse shaping technique for OFDM-based multi-carrier waveform, as shown in Table 2-5:

**Table 2-5 Summary of CP-OFDM with WOLA**

|   | statement   | comments                                   |
|---|---|--|
| 1 | Better side-lobe decay than legacy CP-OFDM              | With Tx-WOLA, as shown in Figure 2-14      |
| 2 | Better suppression of other (async) users' interference | With Rx-WOLA, as shown in Figure 2-15      |
| 3 | Simple implementation using time domain windowing       | Independent of users' allocated bandwidth. |
| 4 | Easy integration with MIMO                              | Same as legacy CP-OFDM                     |

### 2.2.3 UFMC

Like WOLA, UFMC[17] aims to reduce the OOB leakage from the signal. However, while WOLA introduces a raised-cosine prototype filter  $p(n)$  for this, UFMC introduces a non-trivial band-pass filter  $b(n)$ . Figure 2-17 shows the modulator and demodulator for UFMC.

The transmitter operation is shown in Figure 2-18. IFFT symbols are generated in the same way as legacy CP-OFDM. Instead of CP, a guard interval (GI) filled with zeros is introduced between the IFFT symbols to prevent ISI due to tx filter delay. Finally, the symbols go through the tx filter  $b(n)$ , and then transmitted. Usually, the tx filter length is set to be the same as guard interval duration.

Figure 2-19 shows the receiver operation. Since GI is introduced instead of CP, the cyclic convolution property is not preserved in UFMC. Therefore, the receiver structure is not as simple as the one in CP-OFDM. Unlike CP-OFDM receiver which discards CP, UFMC receiver uses whole symbol including GI. For this, 2x size FFT is used at the receiver, but only the even tones of the 2x size FFT outputs are used for the detection. In [17], it is also claimed that the UFMC performance can outperform that of legacy CP-OFDM, since it fully utilizes all the received signals without discarding CP.

Thus, from the point of Figure 2-12, UFMC can be summarized as follows.

In UFMC:

- The prototype filter  $p(t)$  is rectangular pulse followed by zero interval. The zero interval represents the guard interval between the symbols. The rectangular part corresponds to IFFT symbols.
- The tx filter  $b(t)$  is carefully designed to suppress OOB interference. The filter taps for the tx filter  $b(t)$  is usually set to be the same as GI length.

To suppress OOB interference, the tx filter has to be carefully desinged as a band-pass filter which only passes the assigned RB. Especially, when each RB consists of the same number of consecutive tones, the same filter can be universally reused only by shifting the center frequency. The transmitter in Figure 2-17 shows the resulting block diagram. Each RB has the corresponding tx filter. Thus, when  $n$  resource blocks are assigned to the transmitter,  $n$  parallel IFFT and  $n$  tx filtering operations have to be computed in parallel.

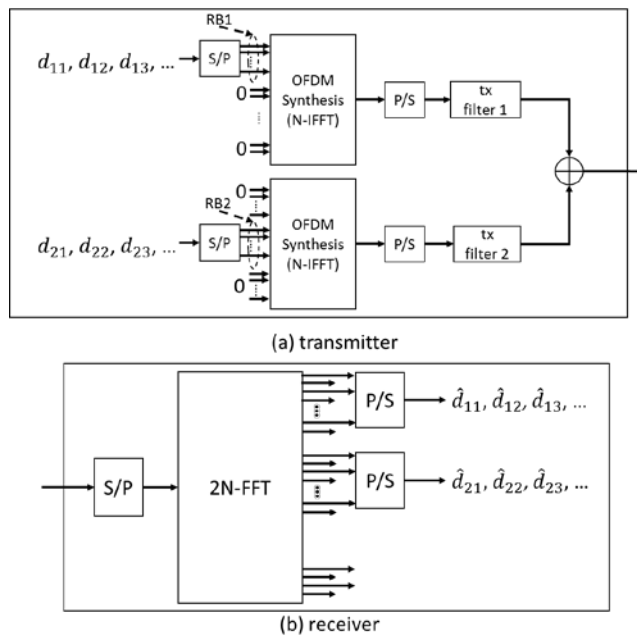


**Figure 2-17 UFMC modulator & demodulator**

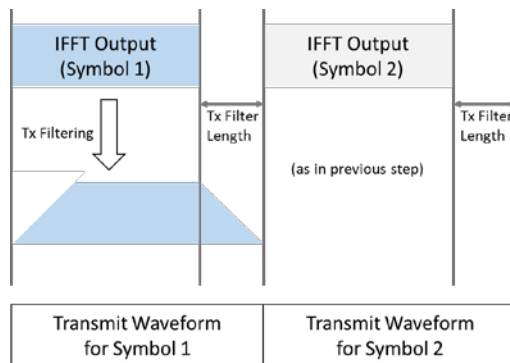


**Figure 2-18 UFMC processing at the transmitter**

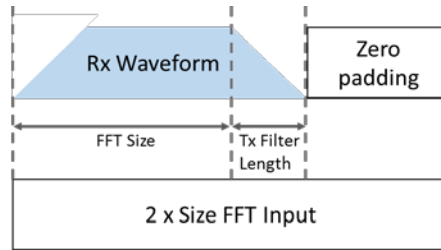


**Figure 2-19 UFMC processing at the receiver**

The remaining issue for UFMC is designing tx filter  $b(t)$  for one RB. In [17], it is chosen as Chebyshev filter or designed to be the one that maximizes signal to out-of-band interference ratio. Figure 2-20 shows the resulting PSD of UFMC when Chebyshev filter is used for the tx filter. FFT and RB sizes are set to be 1024 and 12 respectively. Chebyshev filter has 102 taps, which corresponds to 10% CP, and has 60 dB of relative sidelobe attenuation.

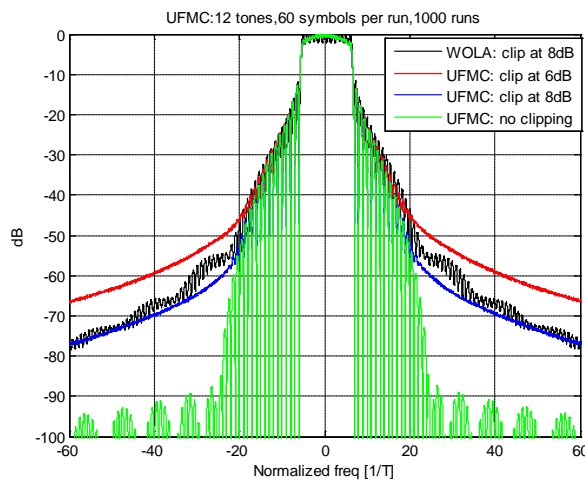


**Figure 2-20 PSD of UFMC with Clipping at Transmitter**

Due to the tx filter and absence of a CP, we can expect that UFMC will suffer from inter-symbol interference over time. However, [17] does not show a clear solution for this. Moreover, as we saw in Figure 2-17, the receiver requires twice the FFT size, which increases complexity and latency of the decoder. Based on the above analysis, we can summarize the following for UFMC:

**Table 2-6 Summary of UFMC**

|   | statement  | comments  |
|---|--|---|
| 1 | Better OOB suppression than legacy CP-OFDM [5]                   | However, the OOB suppression is comparable to CP-OFDM with Tx-WOLA, as in Figure 2-20 |
| 2 | multiplex users with different numerology due to OOB suppression | Similar argument also hold true for CP-OFDM with Tx-WOLA                              |
| 3 | Similar spectral efficiency as CP-OFDM                           | Replacy CP with transitional interval of tx filter.                                   |
| 4 | More complexity at transmitter                                   | Number of IFFT proportional to allocated RB's   |
| 5 | More complexity at receiver                                      | 2x FFT size as in Figure 2-17   |
| 6 | Subject to ISI   | Due to lack of CP   |

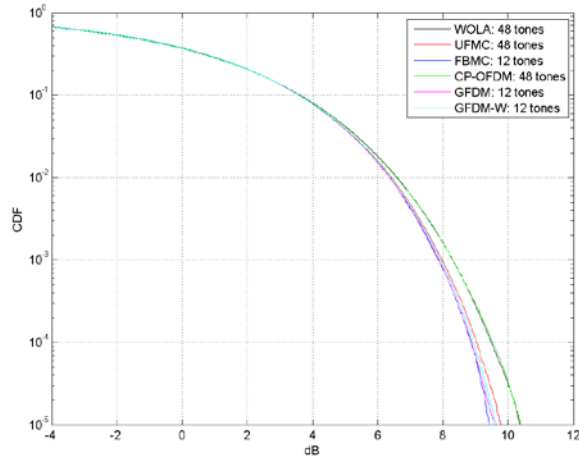


**Figure 2-21 PAPR of different Modulation Schemes**

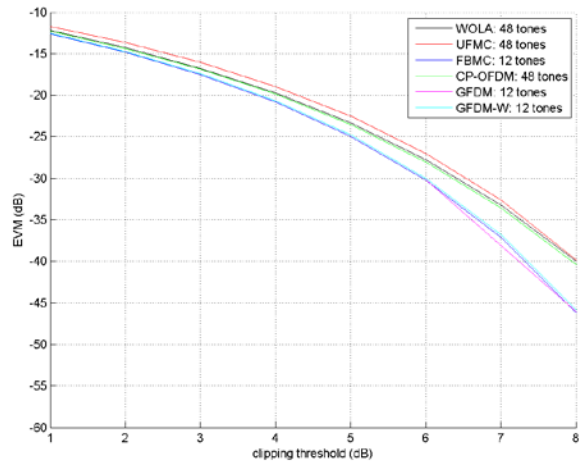


**Figure 2-22 EVM for different Modulation Schemes**

## 2.2.4 FCP-OFDM

One proposal that is similar to UFMC is the flexible CP-OFDM (FCP-OFDM) [18]. The main difference from UFMC is that the overall ZP is split into ZP and CP with flexible partition. The motivation is to provide flexible trade-off between multipath handling and OOB emission suppression.

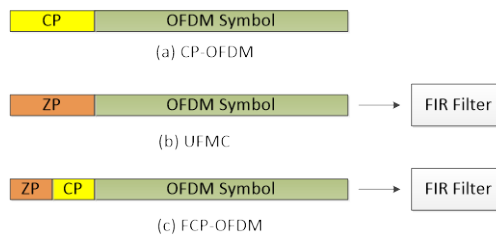


**Figure 2-23 FCP-OFDM**

Figure 2-23 illustrates the difference of symbol structure among legacy CP-OFDM, UFMC and FCP-OFDM. Due to the similarity of FCP-OFDM and UFMC, most of the pros and cons discussed in section 2.2.4 also apply to FCP-OFDM.

## 2.2.5 F-OFDM

Similar as UFMC, filtered-OFDM (F-OFDM) [19] is another spectrum shaping technique utilizing the filtering approach. The main difference is how the band-pass filter is constructed. In UFMC:

- The prototype filter  $p(t)$  is rectangular pulse covering the OFDM symbol as well as CP.
- The tx filter  $b(t)$  is carefully designed to suppress OOB interference.

In [19], the length of the tx filter  $b(t)$  is set to be half of OFDM symbol length. To be specific, the tx filter is computed as the product of ideal band pass filter and a time domain mask:

$$f(n) = p_i(n) \cdot w(n)$$

### Equation 2-2

Here  $p_i(n)$  is the ideal band pass filter covering the allocated bandwidth of the  $i$ -th user, and  $w(n)$  is the Hanning window with length equal half of the OFDM symbol. The long filter length of  $f(n)$  provides good OOB emission suppression, as shown in Figure 2-24.

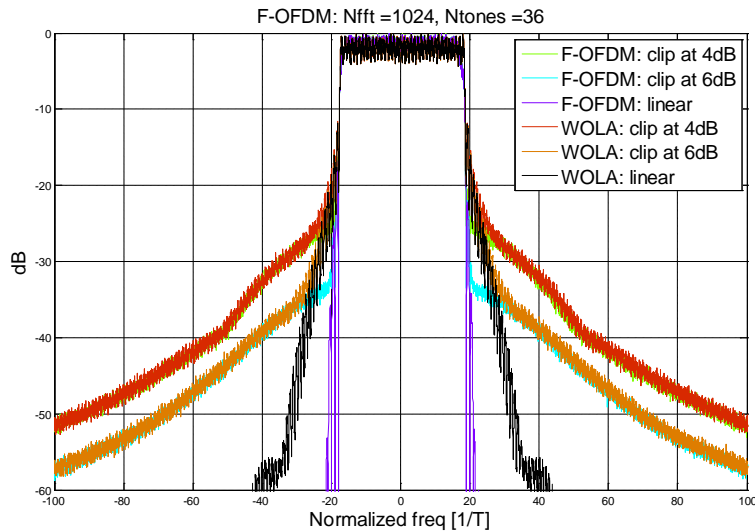


**Figure 2-24 PSD comparison of F-OFDM and WOLA with clipping at transmitter**

As illustrated by Figure 2-24, with non-linearity at transmitter, the OOB emission suppression is degraded (for both F-OFDM and WOLA) compared to the ideal linear scenario. With clipping at 6dB, the OOB emissions are generally comparable between F-OFDM and WOLA, except for a few edge tones.

Different from WOLA (or other pulse-shaping schemes based on windowing approach), the band pass filter of F-OFDM is bandwidth dependent. Therefore the filters will need to be dynamically constructed (or selected) based on the tone allocation. Since the total filter length is fixed, the OOB suppression and ISI effect caused by the filter are also varying depending on the tone allocation.

Another potential concern of applying F-OFDM to applications requiring low latency, especially for TDD band, is the long group delay due to the long filter length. The concatenated transmit and receive filter in [19] requires a processing delay of 1 OFDM symbol. This large processing delay can lead to substantial switching overhead for TDD band.

**Table 2-7 Summary of F-OFDM**

|  | statement | comments |
|--|-----------|----------|
|  |           |          |

|   |  |  |
|---|--|--|
| 1 | Better OOB suppression than legacy CP-OFDM | With tx Non-linearity, it is comparable to CP-OFDM with Tx-WOLA, except a few neighbor tones.        |
| 2 | ISI impact                                 | Filter taps change with Tone assignment, which also lead to varying ISI                              |
| 3 | Processing delay                           | Overall group delay $\sim 1$ OFDM symbol. Challenging for low latency service, specifically with TDD |

## 2.2.6 FBMC

Filter bank multi-carrier (FBMC) technology was originally proposed in the 60's [28][29], and recently has drawn interest for various wireless applications such as cognitive radio, mainly due to its excellent spectral containment [30][31].

The well-localized spectral property is achieved through optimizing the shape of the prototype filter  $p(n)$  through oversampled coefficients in frequency domain. Specifically, the oversampling factor  $K$  is denoted as the FBMC overlapping factor. Figure 2-25 shows an example [27] prototype filter with in frequency domain with  $K = 4$ , i.e. the interval between adjacent coefficients is  $\frac{1}{4}\Delta_f$ , where  $\Delta_f = 1/T$  is the sub-channel spacing. The non-zero coefficients are specified in Table 2-8.

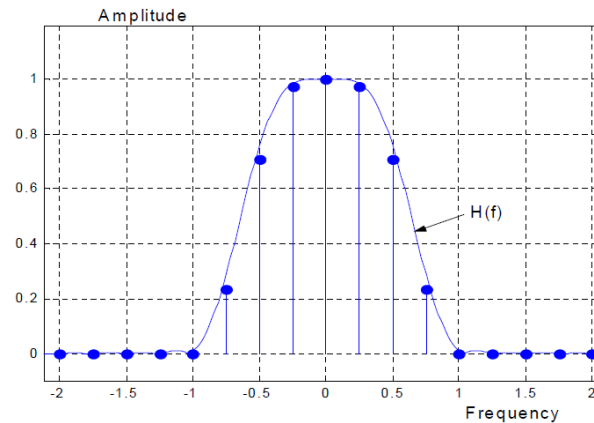


**Figure 2-25 Frequency domain response of prototype filter**

Because of the oversampled frequency coefficients, the prototype filter spans multiple symbol periods  $T$ . Figure 2-26 shows the time domain response of the FBMC prototype filter given by Table 2-8. As reference, we also plot the time domain windowing function for legacy CP-OFDM with and without WOLA in the same figure.

**Table 2-8 Frequency domain coefficients of prototype filter**

| $H_3$    | $H_2$        | $H_1$   | $H_0$ | $H_1$  | $H_2$  | $H_3$  |
|----------|--------------|---------|-------|--------|--------|--------|
| 0.235147 | $\sqrt{2}/2$ | 0.97196 | 1     | $=H_1$ | $=H_2$ | $=H_3$ |

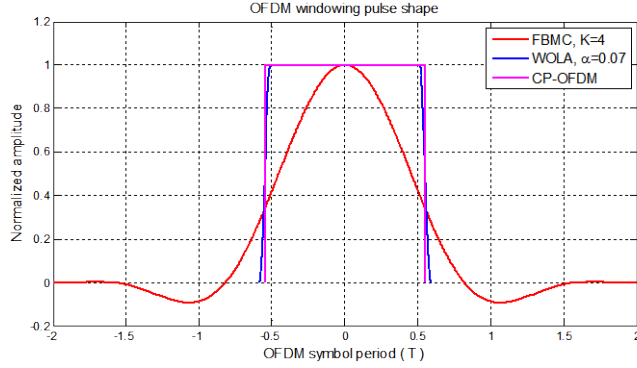


**Figure 2-26 Time domain response of prototype filter**

Therefore, the FBMC waveform again can be synthesized as a special case of Figure 2-12 by

- Setting the prototype filter  $p(n)$  as in Figure 2-26, and
- bypassing  $b(n)$ .

### 2.2.6.1 Equivalence to time-domain windowing

An interesting observation is that the FBMC waveform synthesis is equivalently the “time domain windowing” approach, similar as the WOLA waveform synthesis described in section 2.2.2. Such equivalence is illustrated in [2].

Notice that FBMC waveform synthesis can be efficiently implemented based on polyphase filter network (PPN) as discussed in literature [31][32]. However, modulation and demodulation in FBMC generally have higher complexity than other OFDM waveforms even in systems without MIMO. The complexity increase is partly due to the need of using offset-QAM, as explained in section 2.2.6.2.

### 2.2.6.2 Offset-QAM and orthogonality

A major complication to the FBMC waveform is the potential ISI and ICI. Because each symbol duration spans  $KT$ , in order not to reduce spectral efficiency by  $K$  times, multiple FBMC are overlapped and added in time with offset  $T$  between adjacent symbols. This raises the concern of intersymbol interference at the demodulator.

The FBMC modulator and demodulator are conceptually illustrated in Figure 2-27. To satisfy Nyquist rule, we need the prototype filter  $p(n)$  to be half-Nyquist filter. We can easily verify that the selected frequency coefficients given in Table 2-8 satisfy the half-Nyquist property.

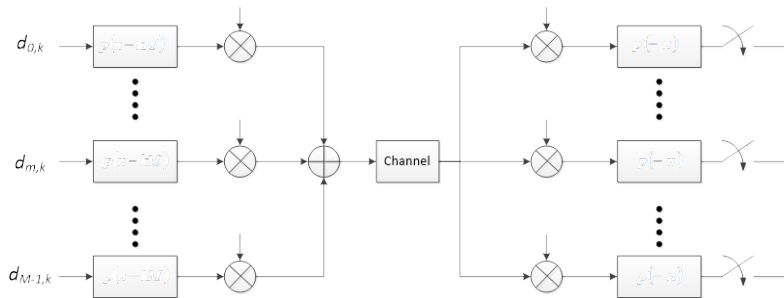


**Figure 2-27 modulator/demodulator of filter bank multi-carrier**

As demonstrated in [2], we can make the following important observations:

- There is no ISI from the same sub-channel, as “demod00” crosses zero at integer multiples of  $T$ . This is due to Nyquist property of the prototype filter.

- There is no ICI between the real part and imaginary part (and vice versa) of two adjacent sub-channels, as the imaginary part of “demod01” crosses zero at integer multiples of  $T$ .
- There is ICI between the real parts (or imaginary parts) of two adjacent sub-channels, as the real part of “demod01” does NOT cross zero at integer multiples of  $T$ . This indicates as long as we alternating between real and imaginary values for the sub-channel input, then there is no ICI at demodulator. However, this reduces spectral efficiency to half of ordinary OFDM waveforms.
- To remove the ICI between the real parts (or imaginary parts) of two adjacent sub-channels, they need to be offset by  $T/2$ . This is shown by “demod01” crosses zero at odd integer multiples of  $T/2$ . This observation motivates “Offset-QAM” (OQAM). The concept of OQAM waveform synthesis is illustrated in Figure 2-28.
- Any ICI/ISI from sub-channels further than the direct adjacent sub-channel is mostly negligible, as shown by the fact that “demod02” is uniformly upper bounded by -60dB across the demod sampling delays<sup>1</sup>. This is a very interesting observation, indicating that FBMC can tolerate asynchronous users even without the use of CP, as long as there is one empty sub-channel between the users.

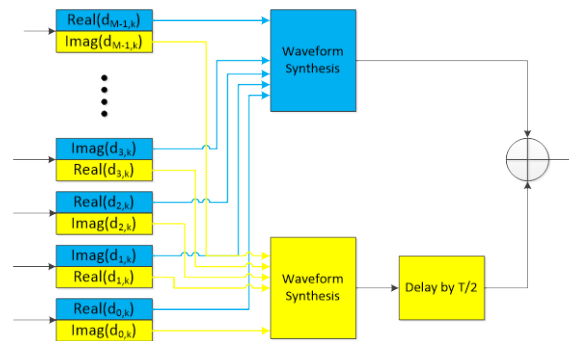


Figure 2-28 FBMC/OQAM waveform synthesis

### 2.2.6.3 Spectral property of FBMC and practical applications

The fundamental benefits of FBMC waveform is the well-localized PSD due to the optimized prototype filter responses. The side-lobe decays much faster than the CP-OFDM, as well as the other multi-carrier waveform options described. Although in practical systems, the benefits of such adjacent channel suppression reduces with PA non-linearity and receiver non-linearity. For example, Figure 2-29 shows the real PSD of FBMC when there is clipping at the transmitter due to PA non-linearity. The prototype filter is selected as given in Table 2-8.

As a fair comparison to other multi-carrier waveforms discussed in previous sections, we normalize the overall FBMC symbol duration to  $T$ , same as the OFDM symbol duration in other waveforms, such that the demod group delay is comparable. This effectively expand the frequency response of each sub-channel wider to  $4/T$ . Therefore, the simulation only uses 3 non-zero sub-channels per frame (compared to 12 sub-channels in previous sections), and the PSD is calculated based on auto-correlation of the synthesized waveform spanning 60 FBMC symbols and averaged over 1000 runs. In each run, an average power is computed, and samples with energy exceeding a given threshold above the average power is clipped. Notice that when the clipping threshold is 6dB above average, the OOB leakage is noticeably higher than the no clipping case. However, it is still noticeably better than other multi-carrier waveforms.

The loose requirement on the synchronization between users, as shown in section 2.2.6.2, make FBMC waveform an attractive candidate for asynchronous multi-users scenarios, such as cellular uplink or cognitive radios [28]. However, there is a caveat in such statement. Although ICI/ISI among asynchronous users are negligible (once an empty sub-channel is inserted), in order to capture all the energy of individual user’s signal, ideally we should use separate FFT window to capture the samples when demodulating each individual user, depending on the user’s time offset. This approach would

<sup>1</sup> It can be easily shown that any ICI/ISI from other sub-channels further than the 2<sup>nd</sup> neighbor is much lower than -60dB.

increase the receiver FFT computation by a factor of number of users. In situations that users' are loosely synchronized, i.e. all users' time offsets are within a small window, it would be possible to still use one FFT-window to capture samples for all users with tolerable performance loss. However, when the time offset among users increases beyond certain threshold (say, 100ns), there is noticeable error floor [32] even in the noise free scenarios. Therefore, in the case of "truly" asynchronous multi-users scenarios, there is a penalty of increased processing complexity at receiver side.

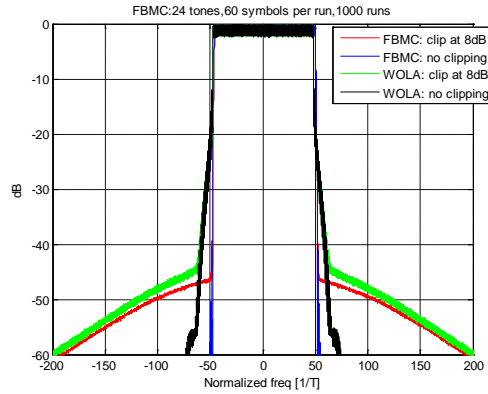


**Figure 2-29 PSD of FBMC with Clipping at Transmitter**

Notice that all the above analysis so far assumes absence of a channel. In the case of multi-path channel, the orthogonality statement at demodulator is no longer valid, since there is no CP protection in the FBMC waveform and channel convolution is not precisely cyclic. To account for channel frequency selectivity at the receiver, equalizer need to be used for demodulation.

Another potential limitation in applying FBMC is the deployment with MIMO when high spectral efficiency is desired by exploiting more degrees of freedom. Compared to the relative straightforward integration with MIMO in CP-OFDM waveforms, integrating MIMO with FBMC is non-trivial [32], due to the interference between adjacent sub-channels. There are existing literature exploiting the feasibility of applying MIMO on FBMC waveforms [31][33], but they all require complicated equalizer and extra processing at receiver. Moreover, the multiplexing of overhead and reference signals may not be as flexible as in CP OFDM or enable as efficient channel estimation techniques.

In addition to the extra processing at transmitter and receiver, FBMC waveform has initial and final pulse transition intervals, as shown in Figure 2-26. Such transition intervals are overhead for the data burst, which are not negligible if the data burst is very short.

Based on the above analysis, we can summarize the following for FBMC:

**Table 2-9 Summary of FBMC**

|   | statement   | comments  |
|---|---|---|
| 1 | Superior side-lobe decay than other MC waveforms [30][31]                         | With non-linearity in practical systems (i.e. PA, receiver,etc), the gap is much smaller. As shown in Figure 2-29                 |
| 2 | FBMC allows users to be async, as long as 1 empty sub-carrier between users [31]. | Receiver need to capture multiple samples with different FFT-window offsets for different users, to avoid lose signal energy [32] |
| 3 | More complicated receiver   | Due to usage of OQAM  |

|   |  |  |
|---|--|--|
| 4 | Nontrivial to integrate with MIMO [30] | Due to usage of OQAM, complicated equalizer need to be used. |
|---|--|--|

### 2.2.6.4 GFDM

Another recent publication [14] that also belong to the category of “multi-carrier waveform with engineered prototype pulse” is the generalized frequency division multiplexing (GFDM). In GFDM, the prototype filter for each sub-carrier is also specifically chosen to be well-localized in frequency domain to reduce ACLR, similar as in FBMC. The main difference from FBMC is that, in GFDM:

- Multiple OFDM symbols are grouped into a block, with a CP added to the block.
- Within a block, the prototype filter is “cyclic-shift” in time, for different OFDM symbols.

A block of GFDM waveform can be expressed as:

$$x(n) = \sum_{k=0}^{K-1} \sum_{m=0}^{M-1} g_{k,m}(n) \cdot d_{k,m} \text{ for } n = 0, 1, \dots, N - 1$$

#### Equation 2-3

Each block has  $N = K \cdot M$  samples, which can be decomposed into  $M$  sub-symbols. Each of the  $M$  sub-symbol contains  $K$  sub-carriers. The pulse  $g_{k,m}(n)$  are the frequency and time shifted version of the prototype filter  $g(n)$ , as shown in Equation 2-4. Specifically, the modulo operation makes  $g_{k,m}(n)$  circularly shifted in time by  $m$  sub-symbols, and the exponential term shifts the filter in frequency by  $k$  sub-carriers.

$$g_{k,m}(n) = g[(n - mK) \bmod N] \cdot e^{j2\pi k \frac{n}{K}}$$

#### Equation 2-4

Figure 2-30 shows an example of GFDM resource partitioning with  $M$  subsymbols per block, with time offset  $\frac{T}{M}$  between adjacent subsymbols. The duration of each symbol can be longer than  $\frac{T}{M}$  due to the specially engineered prototype filter, similar as in FBMC. Each subsymbol contains  $K = \frac{BT}{M}$  sub-channels, with spacing of  $\frac{M}{T}$  (Hz) spacing between adjacent sub-channels.

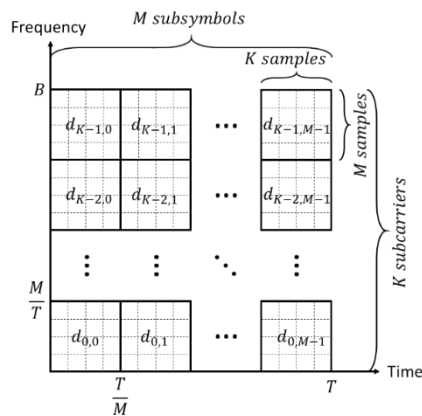


**Figure 2-30 Resource partition in GFDM**

Conceptually, the GFDM can be viewed as a sum of SC-FDM waveforms (assuming the simple case where prototype filter is a rectangle window), where  $d_{k,0}, d_{k,1}, \dots, d_{k,M-1}$  is the data vector for the  $k$ -th SC-FDM waveform. Based on this view,

the GFDM transmitter and receiver can be conceptually illustrated as Figure 2-32. Again, we use the simplified case where prototype filter is a rectangle window.

In order to avoid interference between sub-symbols within a block, the selected prototype filter should have Nyquist property as in FBMC. Further, special modulations such as OQAM may be necessary to avoid inter-channel interference introduced by the prototype, as discussed in section 2.2.6.2. Otherwise, complicated receiver algorithm is needed to handle the interference.

Further, due to the cyclic structure of the block and the use of CP, the GFDM waveform effectively loses the good spectral property of its prototype filter when a waveform spanning multiple blocks in time. This is illustrated in Figure 2-32. To make a fair comparison, we select the prototype filter as used for FBMC in section 2.2.6, which has very sharp side-lobe decay as seen in Figure 2-29. However, the resulting PSD of the GFDM waveform, if without further application of time-domain windowing, is almost comparable as the legacy CP-OFDM. After applying a time-domain windowing, the OOB leakage is much smaller. Therefore, the majority of the OOB suppression is due to the same windowing operation, as used by WOLA discussed in section 2.2.2.

Based on above analysis, we can summarize the following for GFDM:

**Table 2-10 Summary of GFDM**

|   | <b>statement</b>  | <b>comments</b>  |
|---|---|--|
| 1 | A general framework to partition the given time/frequency resource based on specific requirements[14] | GFDM has the flexibility of covering regular CP-OFDM (e.g., $M = 1$ ), or SC-FDE (e.g., $K = 1$ ).   |
| 2 | OOB leakage can be improved by prototype filter [14].   | Most of the suppression comes from windowing (similar as Tx-WOLA). Spectrum property of the prototype filter is lost from non-smooth transition between blocks, as shown in Figure 2-32. |
| 3 | Prototype filter may require more complicated modulation/receiver, e.g. OQAM, similar as in FBMC.     | Maybe can get rid off special prototype filter, as it gives no obvious benefit in OOB suppression.   |

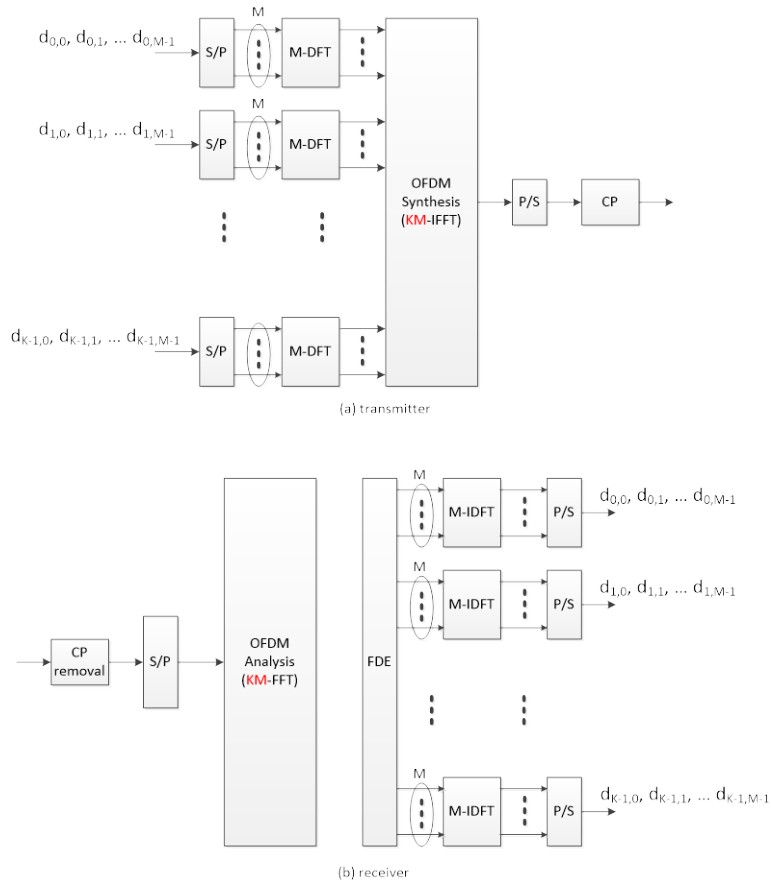


**Figure 2-31 GFDM modulator and demodulator with rectangle pulse shaping**

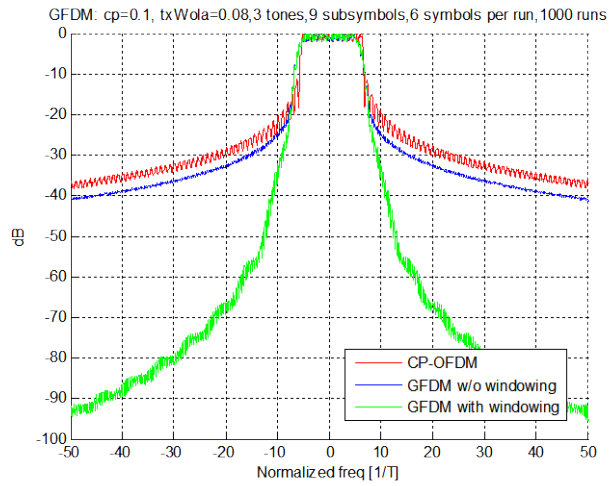


**Figure 2-32 PSD of GFDM with and without windowing**

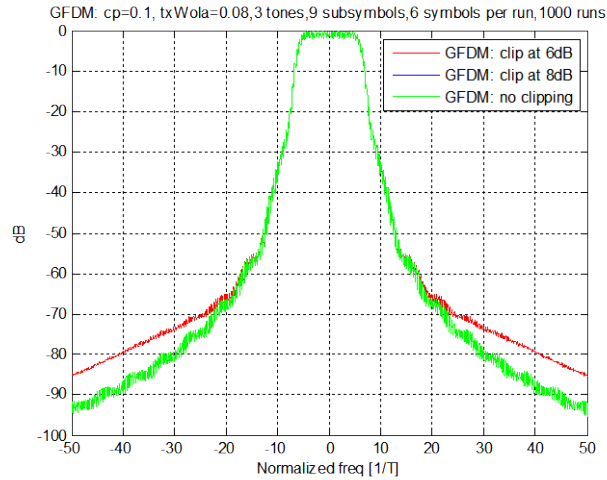


Figure 2-33 PSD of GFDm with windowing for different clipping at transmitter

### 2.2.6.5 Summary of waveform synthesis implementation

In general, most of FFT/IFFT based waveform synthesis can be practically implemented based on the diagram shown in Figure 2-34. Note that “zero-tail” is essentially a guard sequence of zeros prior to the waveform synthesis blocks, while “zero-guard” refers to post-fix of zeros and “CP” is the standard cyclic prefix constructed from the tail of the IFFT block output. The zero-guard absorbs the filter delay imposed by UFMC, as shown in a previous section.

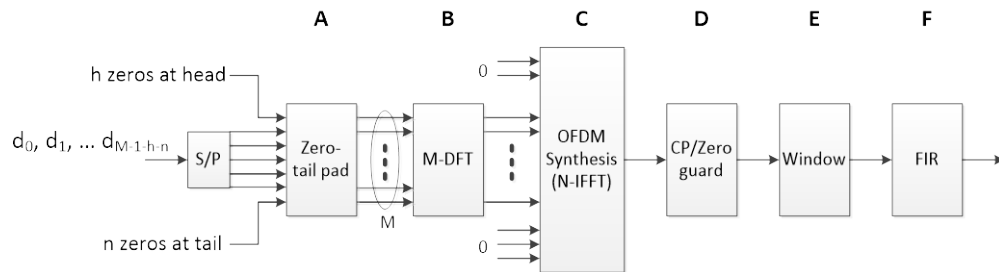


Figure 2-34 Waveform synthesis using FFT/IFFT

Notice that for a specific waveform synthesis, certain blocks are simply bypassed depending on the waveform to be synthesized. To compare the implementation of different waveform synthesis, we summarize in Table 2-11 which blocks are skipped/enabled for individual waveform, respectively.

Table 2-11 Waveform synthesis implementations

| Waveform           | A         | B           | C    | D             | E         | F          |
|--------------------|-----------|-------------|------|---------------|-----------|------------|
|                    | zero tail | DFT-precode | IFFT | CP/Zero-guard | windowing | FIR filter |
| SC-FDM w/ WOLA     | ×         | √           | √    | CP            | √         | ×          |
| Zero-tail DFT-OFDM | √         | √           | √    | ×             | ×         | ×          |

|               |   |   |   |         |   |   |
|---------------|---|---|---|---------|---|---|
| OFDM w/o WOLA | × | × | √ | CP      | × | × |
| OFDM w/ WOLA  | × | × | √ | CP      | √ | × |
| UFMC          | × | × | √ | ZP      | × | √ |
| FCP-OFDM      | × | × | √ | ZP + CP | × | √ |
| FBMC          | × | × | √ | ×       | √ | × |

---

### 3 Conclusions

The following summarizes the proposals in this contribution.

**Proposal 1:** Single carrier waveforms listed in section 2.1 should be evaluated for the potential application of mMTC (WAN IoT) uplink as well as eMBB uplink for macro-cell deployment, based on principles listed in [4].

**Proposal 2:** OFDM-based multi-carrier waveforms listed in section 2.2 should be evaluated for the potential application of eMBB and uLLRC (MiCr) applications, in both uplink and downlink, based on principles listed in [4].

---

### 4 References

[1] “5G White Paper”, Next Generation Mobile Networks (NGMN) Alliance, March 2015. Available at <http://ngmn.org/home.html>

[2] “On Waveform Design for 5G”: <https://www.qualcomm.com/documents/5g-waveform-multiple-access-techniques>

[3] 3GPP R1-162198 “Waveform Requirements for Different Use Cases”

[4] 3GPP R1-162200 “Waveform Evaluation Proposals”

[5] “Waveform contenders for 5G - OFDM vs. FBMC vs. UFMC”, F. Schaich, T. Wild, *Alcatel-Lucent*, 6th International Symposium on Communications, Control and Signal Processing (ISCCSP), May 2014.

[6] “What will 5G be?” J. Andrews, S. Buzzi, W. Choi, S. Hanly, A. Lozano, A. Soong, J. Zhang, *IEEE Journal On Sel. Areas in Comm.*, Vol. 32, No. 6, June 2014.

[7] “Power amplifier linearization with digital pre-distortion and crest factor reduction,” R. Sperlich, Y. Park, G. Copeland, and J.S. Kenney, *Microwave Symposium Digest, 2004 IEEE MTT-S International*, Vol. 2, June 2004.

[8] “[Impact of PA non-linearity on the performance of SCFDM and OFDM for mmW channel](#)”, Qualcomm Internal - Skyber technical review, July 2015.

[9] “[5G Wide Area IOE - Stage 1 Design Review](#)”, Qualcomm Internal – Pentari design review, Feb. 2015.

[10] “Iterative Precoding of OFDM-MISO with Nonlinear Power Amplifiers”, I. Iofedov, D. Wulich, I. Gutman, *IEEE International Conference on Communications*, June 2015.

[11] *Ultra Low Power Transceiver for Wireless Body Area Networks*, J. Masuch and M. Delgado-Restituto, Springer 2013.

[12] “Channel coding with multilevel/phase signals,” G. Ungerboeck, *IEEE Transactions on Information Theory*, Vol 28, Issue 1, 1982.

[13] “Frequency Domain Equalization for Single-Carrier Broadband Wireless Systems,” D. Falconer, S.L. Ariyavisitakul, A. Benyamin-Seeyar, D. Eidson, *IEEE Communications Magazine*, April 2002.

- [14] “Generalized Frequency Division Multiplexing for 5th Generation Cellular Networks,” N. Michailow, M. Matthé, I.S. Gaspar, A.N. Caldevilla, L.L. Mendes, A. Festag, G. Fettweis, *IEEE Transaction on Communications*, Vol. 62, No. 9, September 2014.
- [15] “Performance of FBMC Multiple Access for Relaxed Synchronization Cellular Networks”, J.-B. Dore, V. Berg, D. Ktenas, *IEEE Globecom*, 2014
- [16] “FBMC receiver for multi-user asynchronous transmission on fragmented spectrum”, J.-B. Dore, V. Berg, N. Cassiau, D. Ktenas”, *EURASIP Journal on Advances in Signal Processing*, Vol. 41, March 2014
- [17] X. Wang, T. Wild, F. Schaich, A. Santos, Alcatel-Lucent, “Universal Filtered Multi-Carrier with Leakage-Based Filter Optimization”, *European Wireless 2014*.
- [18] “LGE New RAT Design”, LG Electronics.
- [19] J. Abdoli, M. Jia, J. Ma, “Filtered OFDM: A New Waveform for Future Wireless Systems”, *IEEE 16<sup>th</sup> International Workshop on Signal Processing Advances in Wireless Communications (SPAWC)*, 2015.
- [20] J. G. Proakis, M. Salehi, *Communication Systems Engineering*, Prentice Hall, Inc. Upper Saddle River, New Jersey
- [21] D. A. Guimaraes, “Contributions to the understanding of the MSK Modulation”, *REVISTA Telecommunications*, vol. 11, no. 01, MAIO DE 2008
- [22] K. Murota, K. Hirade, “GMSK Modulation for digital mobile radio telephony”, *IEEE Trans. Comm.* Vol. COM-29, No. 7, July 1981.
- [23] “IEEE standard for local and metropolitan area networks – Part 15.4: low-rate wireless personal area networks (LR-WPANS)”, *IEEE computer society*.
- [24] P. A. Laurent, “Extract and approximate construction of digital phase modulations by superposition of amplitude modulated pulses (AMP)”, *IEEE Trans. Comm.*, vol. COM-34, pp. 150-160, 1986.
- [25] P. Jung, “Laurent’s representation of binary digital continuous phase modulated signals with modulation index  $\frac{1}{2}$  revisited”, *IEEE Trans. Comm.*, vol. 42, no. 2-4, pp. 221-224, 1994.
- [26] F. Khan, “LTE for 4G Mobile Broadband: Air Interface Technologies and Performance”, Cambridge University Press, 2009.
- [27] G Berardinelli, F. M. L. Tavares, T. B. Sorensen, P. Mogensen, K. Pajukoski, Aalborg University/Nokia, “Zero-tail DFT-spread-OFDM Signals”, *IEEE Globecom 2013*.
- [28] R. W. Chang, “High-speed multichannel data transmission with bandlimited orthogonal signals”, *Bell Sys. Tech. J.*, vol. 45, pp. 1775-1796, Dec. 1966.
- [29] B. R. Saltzberg, “Performance of an efficient parallel data transmission system”, *IEEE Trans. Comm. Tech.* vol. 15, no. 6, pp. 805-811, Dec. 1967.
- [30] B. Farhang-Boroujeny, “OFDM versus filter bank multicarrier: development of broadband communication systems”, *IEEE Signal Proc. Magazine*, pp. 92-112, May 2011.
- [31] M. Bellenger, “FBMC physical layer: a primer”, *Phydyas report*, 2010
- [32] J. Fang, Z. You, J. Li, R. Yang, I.T. Lu, “Comparisons of filter bank multicarrier systems”, *System, Applications and Technology Conference*, IEEE long island, May 2013, pp. 1-6.
- [33] M. Najar, C. Bader, F. Rubio, E. Kofidis, M. Tanda, J. Louveaux, M. Renfors, D. L. Ruyet, “MIMO channel matrix estimation and tracking”, *PHYDYAS deliverables D4.1*, Jan. 2009.
- [34] “[White Paper on 5G Concept](#)”, *IMT-2020 (5G) Promotion Group Release Ceremony*, Feb. 2015
- [35] “How to Improve OFDM-like Data Estimation by Using Weighted Overlapping”, C.V. Sinn, *11<sup>th</sup> International OFDM Workshop*, 2006.
- [36] “[5G Design Across Services](#)”, *Johannesberg Summit, Stockholm*, May 2015.
- [37] A. El Gamal, Y. Kim, “*Network Information Theory*”, Cambridge University Press, 2011.